Stem Cell Reports
Resource
OPEN ACCESS

piggyBac Insertional Mutagenesis Screen Identifies a Role for Nuclear RHOA in Human ES Cell Differentiation

Sophia Gayle,[1] Yukun Pan,[1] Sean Landrette,[1] and Tian Xu[1,*]
[1]Howard Hughes Medical Institute and Department of Genetics, Yale University School of Medicine, New Haven, CT 06520, USA
*Correspondence: tian.xu@yale.edu
http://dx.doi.org/10.1016/j.stemcr.2015.03.001

SUMMARY

The mechanisms regulating human embryonic stem (ES) cell self-renewal and differentiation are not well defined in part due to the lack of tools for forward genetic analysis. We present a *piggyBac* transposon gain of function screen in human ES cells that identifies *DENND2C*, which genetically cooperates with *NANOG* to maintain self-renewal in the presence of retinoic acid. We show that DENND2C negatively regulates RHOA activity, which cooperates with NANOG to block differentiation. It has been recently shown that RHOA exists in the nucleus and is activated by DNA damage; however, its nuclear function remains unknown. We discovered that RHOA associates with DNA and that DENND2C affects nuclear RHOA localization, activity, and DNA association. Our study illustrates the power of *piggyBac* as a cost-effective, efficient, and easy to use tool for forward genetic screens in human ES cells and provides insight into the role of RHOA in the nucleus.

INTRODUCTION

The molecular basis for the self-renewal and differentiation of human embryonic stem (ES) cells is not fully understood. In the mouse, self-renewal depends on the maintenance of a core regulatory network of three transcription factors, Nanog, Oct4, and Sox2, which function as a unit to block differentiation (reviewed in Jaenisch and Young, 2008). Mouse embryos null for any of these factors are incapable of maintaining a pluripotent inner cell mass, and cells destined to become epiblast instead develop into extraembryonic lineages (Avilion et al., 2003; Nichols et al., 1998; Chambers et al., 2003; Mitsui et al., 2003). The involvement of these transcription factors has been more recently extended to human ES cells, as they occupy the promoters of a number of genes shown to be differentially upregulated or repressed in human ES cells versus differentiated cells (Boyer et al., 2005). Unlike mouse ES cells, these three factors do not function as a unit to regulate self-renewal of human ES cells and each represses the differentiation of different cell fates (Wang et al., 2012).

Little is known about the factors working with either NANOG, OCT4, or SOX2 to block lineage specific differentiation in human ES cells. Co-immunoprecipitation experiments have been successfully utilized to detect proteins binding to and cooperating with Nanog, Oct4, and Sox2 in mouse ES cells (Wang et al., 2006; Liang et al., 2008; van den Berg et al., 2010; Mallanna et al., 2010; Pardo et al., 2010). We would like to develop a complementary forward genetic approach to identify genes that cooperate with a factor such as NANOG in regulating important biological processes in human ES cells. A forward genetic approach not only has the power to interrogate the genome in an unbiased fashion, but also has the potential to identify cooperating genes that are either not in the same protein complex or have low transcript or protein abundance.

We have previously shown that the *piggyBac* (*PB*) transposon modified from moth can efficiently transpose in the mouse and human genomes (Ding et al., 2005). Here we present a gain of function screen in human ES cells using *PB* transposon mutagenesis. The transposon is specially designed for identifying genes that cooperate with NANOG to block differentiation and support human ES cell self-renewal. As proof of principle, we show that the screen identified *DENND2C*, whose overexpression is capable of genetic cooperation with *NANOG* to block retinoic acid (RA)-induced differentiation. Further characterization revealed that DENND2C negatively regulates RHOA, affecting the localization, activity, and DNA association of nuclear RHOA.

RESULTS

PB Insertional Mutagenesis Screen in Human ES Cells

The *PB* transposon has been demonstrated to be a useful tool for efficient transgenesis and insertional mutagenesis in both mouse and human immortalized cells (Ding et al., 2005). The transposon can efficiently mediate both loss- and gain-of-function insertional mutagenesis in mice (Ding et al., 2005; Rad et al., 2010; Landrette et al., 2011). Given that *PB* can also mediate efficient gene transfer in human ES cells (Chen et al., 2010), we decided to develop a *PB* vector for insertional mutagenesis screens in human ES cells.

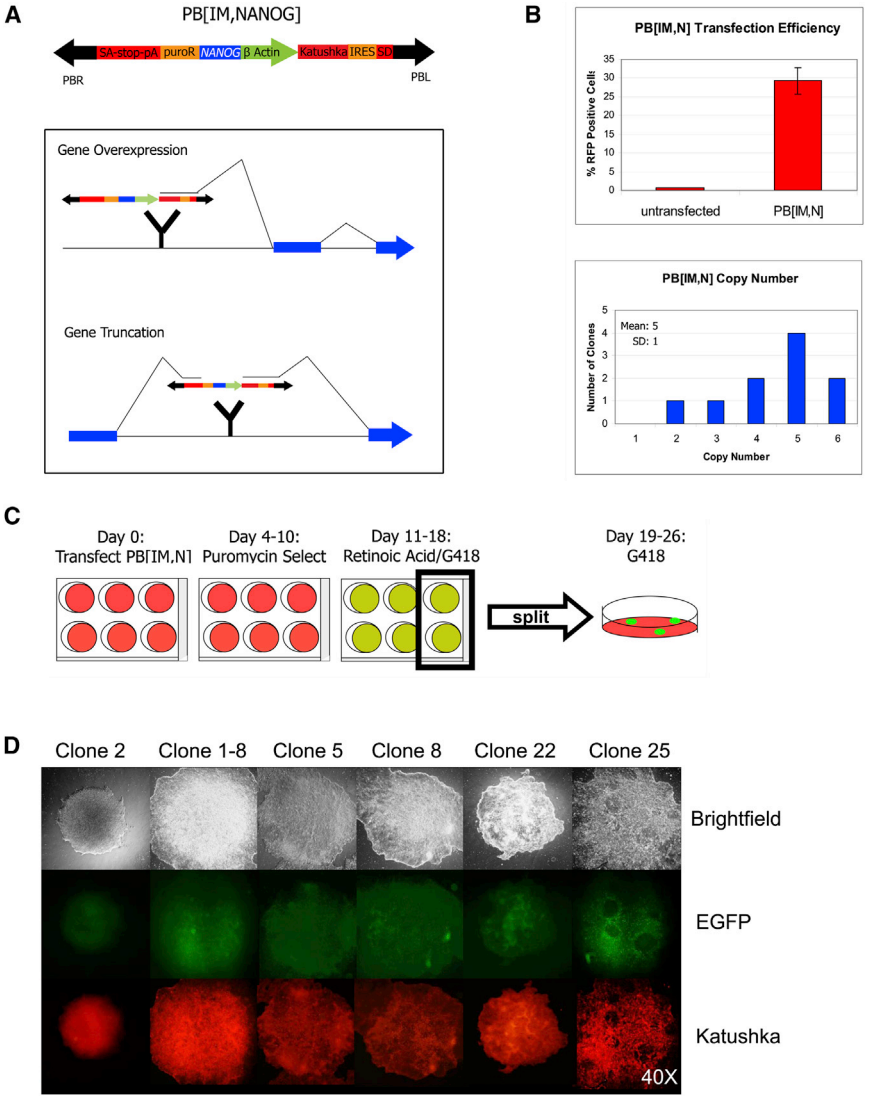

Figure 1. *PB* Mutagenesis in *OCT4* Reporter Human ES Cells

(A) Splicing consequences of PB[Insertional Mutagenesis,NANOG] (PB[IM,N]) insertion either in front of or within the intron of a gene. PB[IM,N] insertion into any reading frame is capable of inducing both overexpression of the downstream transcript with the β actin promoter and triple reading frame start cassette (not shown) as well as simultaneous expression of Katushka fluorescent marker by the splicing of Katushka/IRES into the native transcript with the splice donor (SD). This construct is also able to create N-terminally truncated transcripts with the splice acceptor, triple reading frame stop cassette, and poly A tail (SA-stop-pA). PB[IM,N] can also constitutively overexpress *NANOG* transcript from the independent *NANOG* overexpression cassette.

(B) (Top) FACS analysis of Katushka expression from PB[IM,N] in human ES cells 48 hr after transfection in single-cell suspension using the RFP channel. Mean of triplicate independent experiments is shown. Error bars represent SD. (Bottom) *PB* copy number within ten individual PB[IM,N] transfected human ES cell clones as assessed by real time PCR. There is a mean of five PB[IM,N] insertions per clone.

(C) Protocol of screen performed in H1 *OCT4*-EGFP cells for resistance to RA-induced differentiation using PB[IM,N]. Cells in six-well plates were transfected with PB[IM]N, puromycin selected, and subsequently treated with RA and G418. Cells were then split from the six-well plates into 10-cm plates at a 2:1 ratio and maintained on G418 alone.

(D) Brightfield and fluorescent images of the six unique clones recovered from the screen. All clones are positive for EGFP and Katushka fluorescent reporters for *OCT4* expression and PB[IM,N] insertion within an actively expressed gene.

To identify factors that cooperate with NANOG to block RA-induced differentiation, we have taken the advantage of *PB*'s large cargo capacity to develop an insertional mutagenesis vector that can simultaneously express the *NANOG* transgene (PB[IM,N]; Figure 1A; Ding et al., 2005; Li et al., 2011). PB[IM,N] insertion upstream of a gene results in constitutive overexpression of the downstream gene, while insertion within a transcription unit can result in overexpression of a truncated gene product downstream of the insertion site, leading to constitutive activation, dominant-negative effects, or heterozygous knockout of the gene (Figure 1A). In addition to mutagenesis, such insertions result in fluorescent labeling of mutated cells with Katushka marker. Upon co-transfection with a helper plasmid carrying the *PB* transposase transgene, PB[IM,N] stably integrates into the genome of about 30% of transfected human ES cells with an average of five copies of transposon per genome (Figure 1B; Experimental Procedures). Of 133 *PB* insertions mapped in human ES cells to date, 93% of insertions are within 200 kb of a gene, and 53% are located within an intron. This is consistent with data showing that *PB* frequently integrates near to or within coding units, making this transposon a useful tool for insertional mutagenesis of genes (Ding et al., 2005). The puromycin antibiotic resistance marker within the construct allows for the selection of cells with stable *PB* integration. Thus,

this vector allows one to generate a library of individually mutagenized human ES cells with the condition of NANOG overexpression in a quick, easy, and cost-effective fashion.

For this screen, we have used an H1 human ES cell line containing an EGFP reporter and neomycin resistance cassette knocked into the *OCT4* 3′UTR (Zwaka and Thomson, 2003; H1 *OCT4*-EGFP or WT cells). Undifferentiated cells that continue to express the self-renewal factor OCT4 are both EGFP positive and G418 resistant. We utilized PB[IM,N] to screen for genes capable of genetically cooperating with NANOG to block differentiation of H1 *OCT4*-EGFP human ES cells. For the screen, approximately 9.6×10^7 cells were transfected in single-cell suspension with PB[IM,N] and the *PB* transposase transgene plasmid in 24 Matrigel-coated 6-well plates, allowing for the isolation of individual mutant clones after puromycin selection. Surviving adherent and puromycin selected cells were subsequently treated with a combination of RA and G418 in the same monolayer culture. Six surviving independent clones with undifferentiated morphology were isolated and confirmed in retesting (Figure 1C; see Experimental Procedures for details). All of these Katushka-positive clones express *OCT4*-EGFP, indicating that they remain undifferentiated (Figure 1D).

In human ES cells, the expression of a *NANOG* transgene confers inhibition of spontaneous differentiation and fibroblast growth factor (FGF) independence (Zhang et al., 2009; Darr et al., 2006). In mouse ES cells, expression of a *Nanog* transgene has been shown to confer several effects, including resistance to RA-induced differentiation, leukemia inhibitory factor (LIF) independence, and increased colony formation (Chambers et al., 2003; Mitsui et al., 2003; reviewed in Pan and Thomson, 2007). We confirmed that expression of NANOG by a *PB* vector in the H1 *OCT4*-EGFP cells stabilizes human ES cells to resist spontaneous differentiation (PB[NANOG] or NANOG; Figure 2A). Unlike in mouse ES cells, NANOG overexpression in human ES cells confers only weak resistance to RA-induced differentiation. All WT human ES cells appear morphologically differentiated in response to RA treatment (Figure 2B). This differentiation is reflected by induction of the GATA6 endoderm marker (Figures 2B and 2C). In contrast, NANOG expressing colonies after RA treatment contain small patches of cells that appear morphologically undifferentiated and continue to express NANOG (Figures 2B and 2C). This weak resistance to RA is also observed in cells transfected with the PB[IM,N] mutagenic construct (Figure 2D). Concordant with these results, only a few PB [NANOG] or PB[IM,N] colonies are able to survive when RA treatment is combined with G418, as differentiated cells no longer express the G418 resistance marker (Figure 2E). Thus, NANOG overexpression in human ES cells offers an ideal condition for forward genetics, as the small degree of resistance to differentiation allows for a sensitized screen without the drawback of excessive background. The clones identified from the screen display robust resistance to RA treatment in comparison to NANOG overexpressing escapers (Figure 2E). Indeed, only the identified clones can survive more than one round of RA treatment.

The *PB* insertion sites in the resistant clones were determined by PCR and sequencing (Experimental Procedures; Table S1). Detailed characterization of one of the isolated clones is presented below, while other information will be described elsewhere.

Identification of *DENND2C* as a NANOG Collaborator for Blocking Differentiation

The clones isolated from the screen exhibit varying degrees of blocking RA-induced differentiation and different morphologies, suggesting different underlying mechanisms of resistance (Figure 2E). Clone 2 was of particular interest to us because of its unique morphology. Cells from this clone resisted spontaneous differentiation and instead piled into dense, multilayered colonies, with some cells aggregating into balls. These cells exhibited a weak attachment to Matrigel as they are readily detached after collagenase IV treatment. Clone 2 had three *PB* insertions, the examination of which led to the identification of the causative gene, *DENND2C*. DENND2C belongs to a family of proteins containing DENN domains (Differentially Expressed in Normal versus Neoplastic; reviewed in Marat et al., 2011). A *PB* insertion is located within an intron of the *DENND2C* gene, resulting in the overexpression of the C-terminal DENN domain of the gene while not having significant effects on the expression of surrounding genes (Figure 3A). More importantly, overexpression of the *DENND2C* gene product alone, either truncated or full length, in the NANOG-expressing parental cells phenocopies clone 2 morphology and behavior (Figure 3B). This indicates that *PB* disruption of *DENND2C* is the causative alteration (Figures 3A and 3B).

These cells maintain the expression of stemness markers OCT4, NANOG, and alkaline phosphatase and are able to form well-differentiated teratomas in mice, indicating that they are undifferentiated (Figures 3C, 3D, and S1A). DENND2C expressing cells are resistant to spontaneous differentiation as well as several passages in RA-treated media; however, resistance is not observed with other differentiating agents such as 12-O-Tetradecanoylphorbol-13-acetate (TPA). Furthermore, the effects of DENND2C on colony morphology were reversible in a doxycycline-inducible system (data not shown).

By comparing cells overexpressing either DENND2C alone or DENND2C expressed in the PB[NANOG] background, we discovered that DENND2C alone is responsible

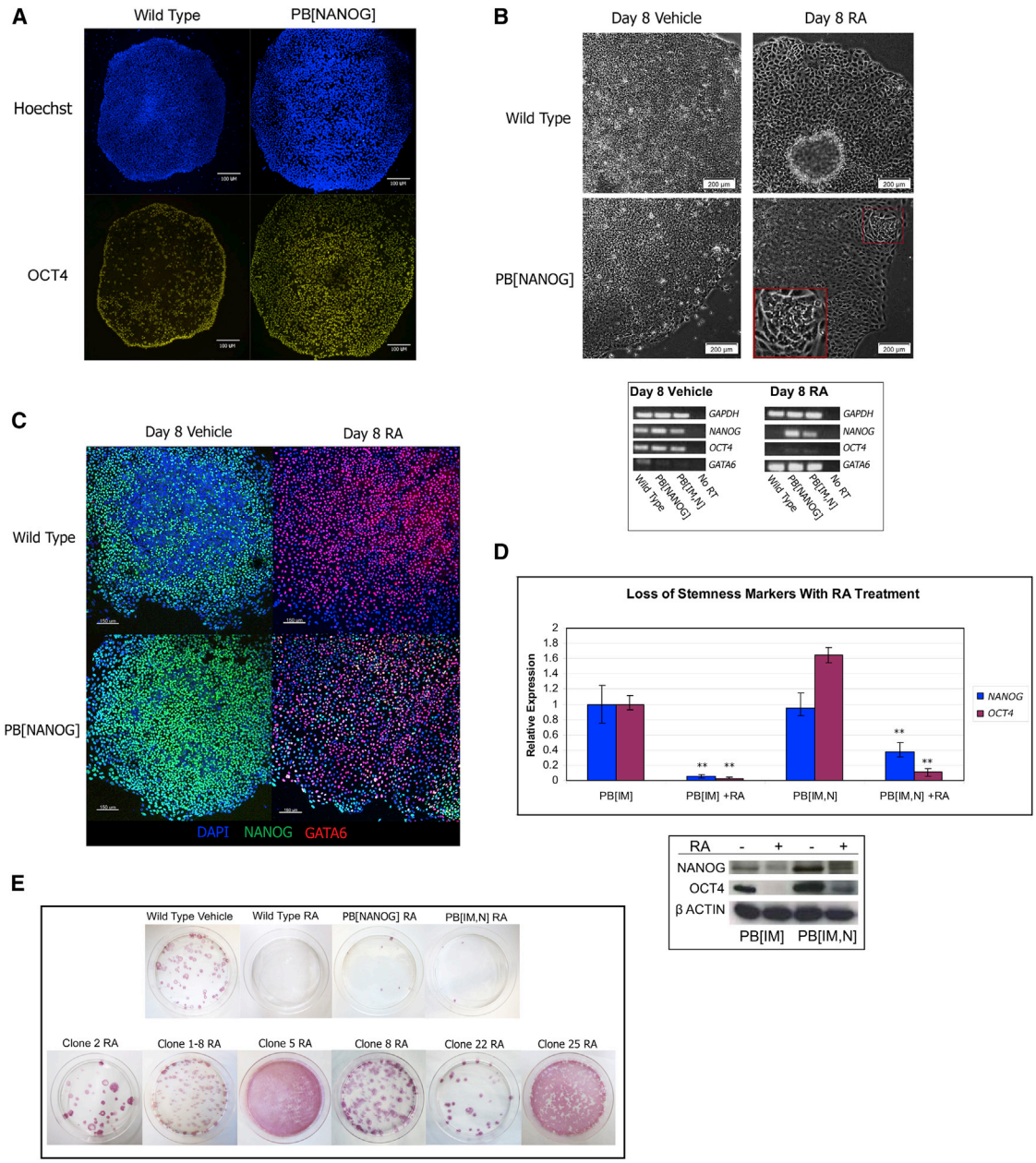

Figure 2. NANOG Expression from *PB* Constructs Induces Resistance to RA-Induced Differentiation

(A) OCT4 immunostaining in WT and NANOG expressing human ES cells. NANOG expressing cells resist spontaneous differentiation and maintain OCT4 signal in colony centers at larger diameters than WT cells. Scale bar represents 100 μm.

(B) (Top) Morphology of RA differentiated cells. The red square highlights a cluster of morphologically undifferentiated NANOG expressing cells after RA treatment, magnified in inset. Scale bar represents 200 μm. (Bottom) RT-PCR analysis of RA-differentiated cells.

(C) Immunostaining of RA-differentiated cells co-stained for NANOG and GATA6. RA induces differentiation of human ES cells as assessed by GATA6 endoderm marker. Scale bar represents 150 μm.

(D) Real-time PCR (top) and western blot (bottom) analysis of stemness marker expression in RA-treated cells. The addition of a NANOG overexpression cassette to PB[IM] induces protein overexpression of both NANOG and the NANOG target OCT4 and induces weak persistence of NANOG and OCT4 after RA treatment. Graph shows mean of triplicate independent experiments. Error bars represent SD. $^{**}p < 0.001$ in Student's t test.

(E) Alkaline phosphatase staining of combined RA/G418-treated cells after 16 days. Experiments are performed in duplicate. A representative plate is shown.

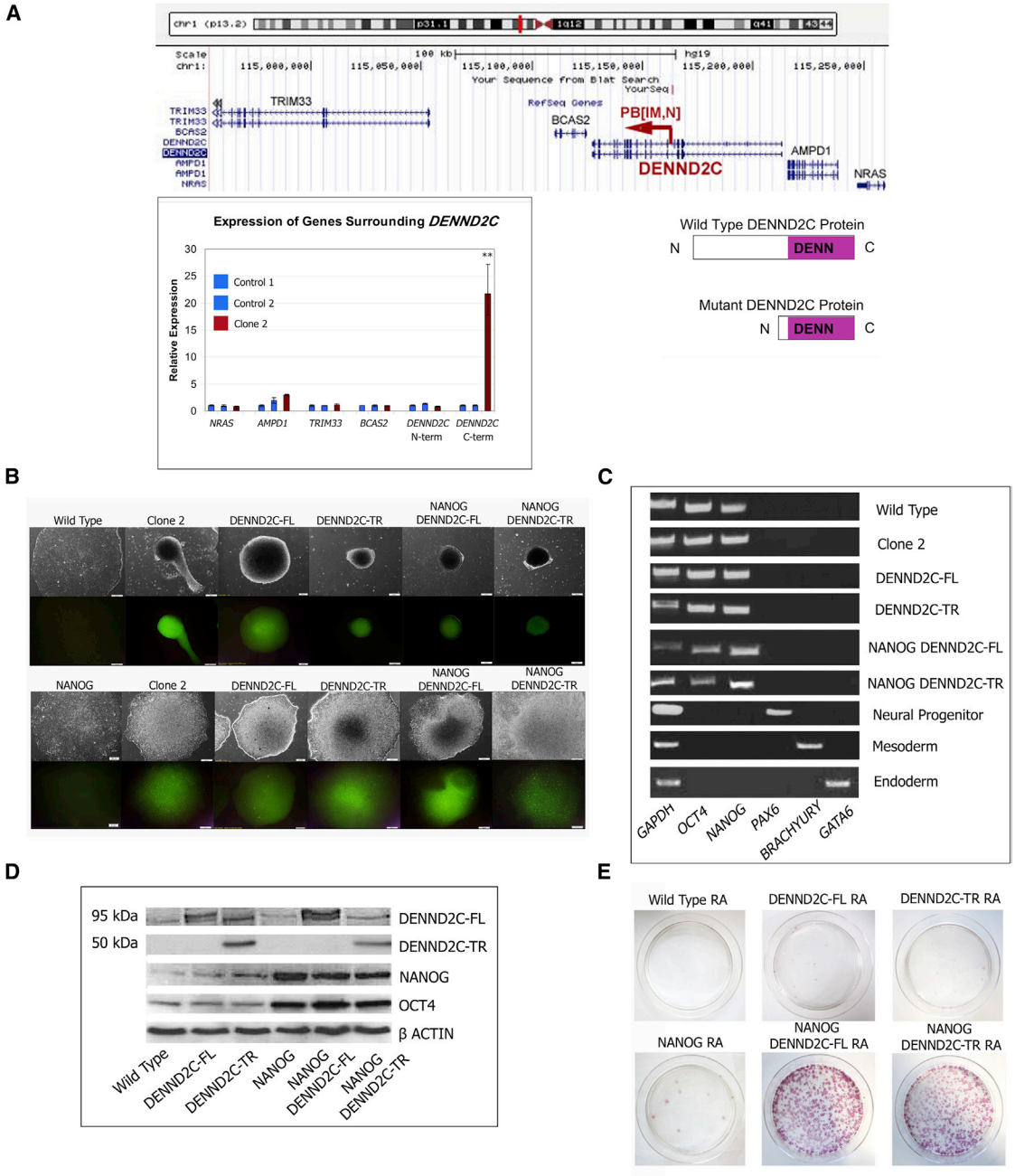

Figure 3. *PB* Mutagenesis of *DENND2C* Causes Morphological Changes and Resistance to RA

(A) (Top) Screenshot from the UCSC Genome Browser detailing the position and orientation of the PB[IM,N] insertion in *DENND2C* mapped in clone 2 (red arrow). (Bottom right) PB[IM,N] insertion results in overexpression of the C-terminal half of DENND2C, made up primarily of its DENN domain. (Bottom left) The C terminus of DENND2C is significantly upregulated in clone 2 by real-time PCR. Graph shows mean of triplicate technical replicates, and error bars represent SD. **$p < 0.001$ in Student's t test.

(B) Brightfield and *OCT4*-EGFP reporter images of clone 2 and DENND2C expressing human ES cells. Clone 2 aggregates into either balls of cells or flat, extremely dense colonies that resist spontaneous differentiation. Cells stably transfected with full-length (FL) or truncated (TR) DENND2C also display this behavior. Scale bar represents 50 μm.

(C) RT-PCR showing maintenance of stemness in DENND2C expressing human ES cells, which do not display markers of differentiation.

(legend continued on next page)

for the morphological properties of clone 2, while cooperation of DENND2C and NANOG is responsible for blocking RA-induced differentiation (Figures 3B and 3E). This genetic cooperation is also observed in induced pluripotent stem cells co-expressing DENND2C and NANOG (Figure S1B).

DENND2C Functions as a Negative Regulator of RHOA and RAC1

DENN domain proteins have been shown to function as RAB GEFs (GDP-GTP exchange factors) as well as interact with non-RAB proteins (Allaire et al., 2010; Yoshimura et al., 2010; reviewed in Marat et al., 2011). The DENND2 subfamily consists of four members, A through D. While all four DENND2 subfamily members could behave as RAB9 GEFs by in vitro GDP release activity, the in vivo functions for DENND2B, DENND2C, and DENND2D are unknown, as only DENND2A knockdown phenocopies the lysosomal defect caused by RAB9 inactivation in HeLa cells (Yoshimura et al., 2010). Consistent with the previous report, we detected a lysosomal defect for DENND2A, but not for DENND2C in knockdown experiments in human ES cells (Figure S1C). Furthermore, deregulation of RAB9A and B activities using dominant-negative and active mutants does not result in any of the ES cell phenotypes caused by DENND2C (Figure S1D). These data indicate that DENND2C does not function as a regulator for RAB9 in human ES cells.

DENND2 proteins are expressed within the nucleus and cytoplasm of both undifferentiated and differentiated human ES cells (Figure S1E). While DENND2C knockdown does not induce differentiation, it is possible that it shares redundant function with other DENND2 proteins. We were unable to induce sufficient simultaneous knockdown of DENND2 proteins to induce differentiation in human ES cells.

We thus further examined the colony morphology phenotype caused by DENND2C, as it could provide clues for underlying molecular mechanisms. DENND2C-expressing colonies have a strikingly disorganized cortical F-actin staining pattern, which differs from the organized cortical F-actin pattern observed in WT human ES cells (Figure 4A). In addition, these cells are smaller in cell and nuclear sizes, which is more dramatic toward the interior of colonies (Figure 4A). Despite these morphological changes, these cells remain actively proliferative with no changes in either DNA content or cell-cycle profile compared with WT human ES cells (Figure S1F).

The striking cytoskeletal and morphological changes in clone 2 and DENND2C-expressing cells suggested that a cytoskeletal regulator could be the potential effector of DENND2C. Thus, we tested components of several pathways regulating the cytoskeleton, cell size, and cell adhesion by stably transfecting *PB* constructs containing WT, dominant-negative, and constitutively active forms of these genes into WT human ES cells. These candidate genes were examined for morphologies similar to DENND2C expressing cells as well as the ability to block RA-induced differentiation when transfected into the PB[NANOG] cell line. We discovered that reduction of RHOA and RAC1 activities by the expression of dominant-negative alleles, knockdown, or direct chemical inhibition could recapitulate the DENND2C-expressing phenotypes. Downregulation of either RHOA or RAC1 causes the cells to pile into dense, multilayer colonies (Figures 4B and S2A–S2F). However, only downregulation of RAC1 results in cells aggregating into balls (Figures 4B and S2A). Expression of dominant-negative RAC1 (T17N, RAC1 DN) results in the small cell and nuclei phenotypes observed in DENND2C-expressing cells (Figure 4C). On the other hand, expression of dominant-negative RHOA (T19N, RHOA DN) results in altered F-actin morphology phenotypes (Figure 4C). Expression of dominant-negative RHOB or RHOC (T19N) does not elicit these morphological changes, instead triggering differentiation (data not shown), indicating that the morphological changes are specific to downregulation of RHOA activity. Finally, similar to clone 2 and DENND2C-expressing clones, cells with reduction of either RHOA or RAC1 activity maintain the expression of stemness markers (Figure S2G).

Although we were unable to test the effects of RAC1 disruption in blocking RA due to its suppression of proliferation, disruption of RHOA exhibits genetic cooperation with NANOG expression in a manner similar to DENND2C to block RA-induced differentiation (Figures 4D and S2D). This genetic cooperation enhances NANOG-induced repression of the endoderm differentiation trigger GATA6 (Figure 4E; Capo-Chichi et al., 2005; Cai et al., 2008).

As it has been shown that chemical inhibition of the RHOA effector ROCK with the drug Y-27632 (ROCK inhibitor) results in resistance to RA, we wondered whether ROCK inhibitor treatment of NANOG expressing cells

(D) Western blot demonstrating that DENND2C overexpressing cells produce NANOG and OCT4 proteins at levels comparable to the parental WT and NANOG overexpressing cell lines. Overexpressed DENND2C-FL runs as a doublet, while only DENND2C-TR lysate exhibits a band running at the predicted 50 kDa of truncated DENND2C.

(E) Alkaline phosphatase-stained plates after RA/G418 treatment. Experiments were performed in triplicate. A representative plate for each set of experiments is shown.

See Figure S1 for additional information.

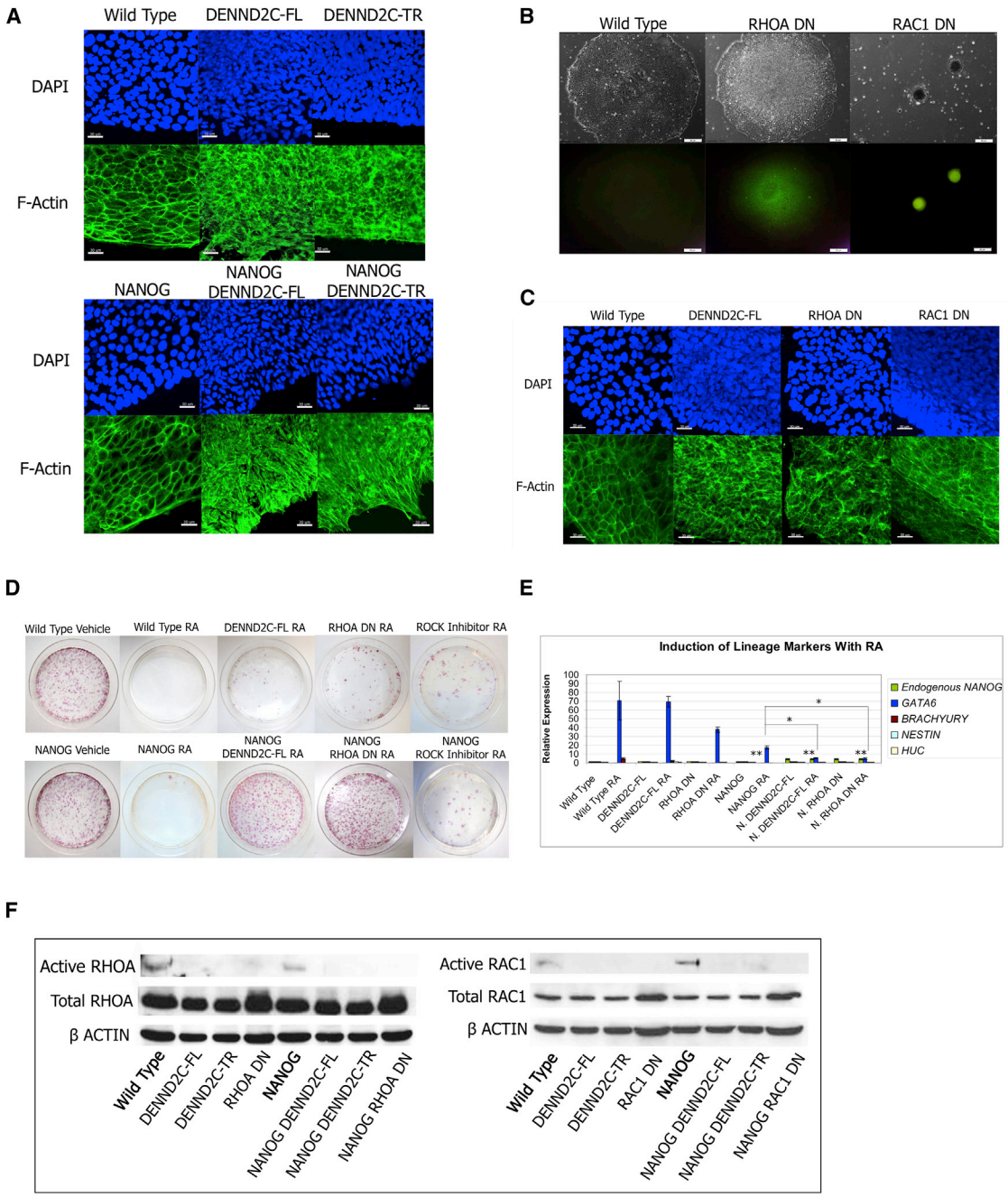

Figure 4. DENND2C Phenotype Is Induced by Loss of Active RHOA and RAC1

(A) DAPI and F-actin immunostaining of WT and DENND2C expressing human ES cells. Scale bar represents 30 μm.

(B) Brightfield and *OCT4*-EGFP reporter images of cells stably expressing dominant-negative RHOA T19N (RHOA DN) and dominant-negative RAC1 T17N (RAC1 DN). Scale bar represents 50 μm.

(C) DAPI and F-actin immunostaining of WT and RHOA DN and RAC1 DN mutant human ES cells. Scale bar represents 30 μm.

(D) Plates stained for alkaline phosphatase after RA/G418 treatment. Experiments were performed in triplicate. A representative plate for each set of experiments is shown.

(E) The induction of lineage markers with RA assessed by real-time PCR. RA treatment induces differentiation as reflected by the induction of the endoderm marker GATA6. NANOG expression from *PB* induces some repression of GATA6 and no upregulation of endogenous NANOG. NANOG/DENND2C and NANOG/RHOA DN cells display enhanced repression of GATA6 and upregulation of

(legend continued on next page)

could block RA-induced differentiation (Krawetz et al., 2011). However, unlike Rho inhibitor treatment, ROCK inhibitor treatment does not cooperate with NANOG to block RA-induced differentiation (Figures 4D and S2D). Given that NANOG overexpression also results in the overexpression of its target OCT4, we further wondered whether OCT4 overexpression could cooperate with RHOA disruption to block RA-induced differentiation. However, this was not the case (Figure S2H). These results indicate that our approach of NANOG sensitized *PB* mutagenesis is useful in identifying relevant genetic interactions with NANOG capable of blocking RA-induced differentiation.

Inactivation of RHOA and RAC1 recapitulates DENND2C-expressing phenotypes and suggests that DENND2C could be a negative regulator of RHOA and RAC1. We next examined the possibility that DENND2C physically interacts with RHOA and RAC1; however, we did not detect such interactions by co-immunoprecipitation (data not shown). We thus directly examined the activities of RHOA and RAC1 in human ES cells expressing either full-length or truncated DENND2C by immunoprecipitation of the active forms of these GTPases. Indeed, in both cases, overexpression of DENND2C results in decreased levels of active RHOA and RAC1 (Figure 4F).

DENND2C Affects Nuclear RHOA Function

Given that DENND2C negatively regulates RHOA activity, we examined whether DENND2C expression affected RHOA localization. Interestingly, while WT cells displayed RHOA staining throughout the cell, in DENND2C expressing cells, RHOA was relocalized away from the interior of the nucleus (Figure 5A). Although RHOA plays an essential role in the regulation of cytoskeleton dynamics, many of the known functions of RHOA relate to its functions in the cytoplasm (reviewed in Burridge and Doughman, 2006). RHOA has been recently documented to reside in the nucleus (Dubash et al., 2011). In fact, actin and many actin nucleators have also been found in the nucleus, implicating functional significance for the nuclear cytoskeleton (reviewed in de Lanerolle, 2012; Weston et al., 2012; Hofmann, 2009). While it has been shown that nuclear RHOA is activated in response to DNA damage, its function within the nucleus remains unknown (Dubash et al., 2011).

We therefore examined whether DENND2C affected the localization and activity of nuclear RHOA. By immunostaining human ES cell nuclei isolated by density gradient centrifugation, it was evident that WT and NANOG overexpressing cells contained RHOA throughout the nucleus (Figure 5B). In contrast, RHOA in DENND2C overexpressing nuclei is relocalized to the nuclear periphery (Figure 5B). We next examined the activity of RHOA in nuclear and cytoplasmic fractions of WT and DENND2C expressing human ES cells (Guilluy et al., 2011). In addition to reduced cytoplasmic RHOA activation, DENND2C expressing cells have significant reduction of nuclear RHOA activation (Figure 5C). We observed similar reduction of active nuclear RHOA in the RHOA DN-expressing positive control (Figure 5C).

As a negative control, we expressed RAB35 in human ES cells, which has been implicated in the cytoplasmic transport and regulation of Rho GTPases (Chevallier et al., 2009; Shim et al., 2010). Indeed, expression of RAB35 inhibits cytoplasmic RHOA activity, but not nuclear RHOA activity, nor does RAB35 expression result in cooperation with NANOG in blocking RA-induced differentiation (Figures 5C and S3A–S3E). Furthermore, the expression of RHOA DN tagged with a nuclear exclusion signal does not cooperate with NANOG to block differentiation (Figure S3F). Together, our data suggest that DENND2C downregulates both nuclear and cytoplasmic RHOA activity, which cooperates with NANOG to block RA-induced differentiation. Indeed, nuclear RHOA is hyperactivated during RA-induced differentiation of WT human ES cells, supporting this hypothesis (Figure S3G).

Given that DENND2C negatively regulates nuclear RHOA, we wondered what function RHOA had within the nucleus. Other cytoskeletal effectors are known to associate with DNA either globally or with certain promoters when activated, and furthermore, nuclear RHOA is activated in response to DNA damage (Mazumdar et al., 2011; Buongiorno et al., 2008; Dubash et al., 2011). We therefore hypothesized that nuclear RHOA may associate with DNA. Using chromatin immunoprecipitation (ChIP) with an anti-RHOA monoclonal antibody that works well for immunoprecipitation (Figure S3H), we were able to pull down large amounts of DNA in undifferentiated WT and NANOG expressing human ES cells (Figure 5D). In contrast, the amount of DNA associated with RHOA in DENND2C overexpressing human ES cells is dramatically reduced (Figure 5D). The RHOA-precipitated DNA includes the *OCT4* and *GATA6* promoters, DNA from a gene desert located on chromosome 13, as well as

endogenous NANOG at the RNA level. Graph shows mean of triplicate independent experiments. Error bars represent SD. $^{**}p < 0.001$, $^{*}p < 0.05$ in Student's t test.

(F) Immunoprecipitation of active RHOA and RAC1 in DENND2C expressing cells. DENND2C expressing cells have decreased active RHOA and RAC1 relative to WT cells.

See Figure S2 for additional information.

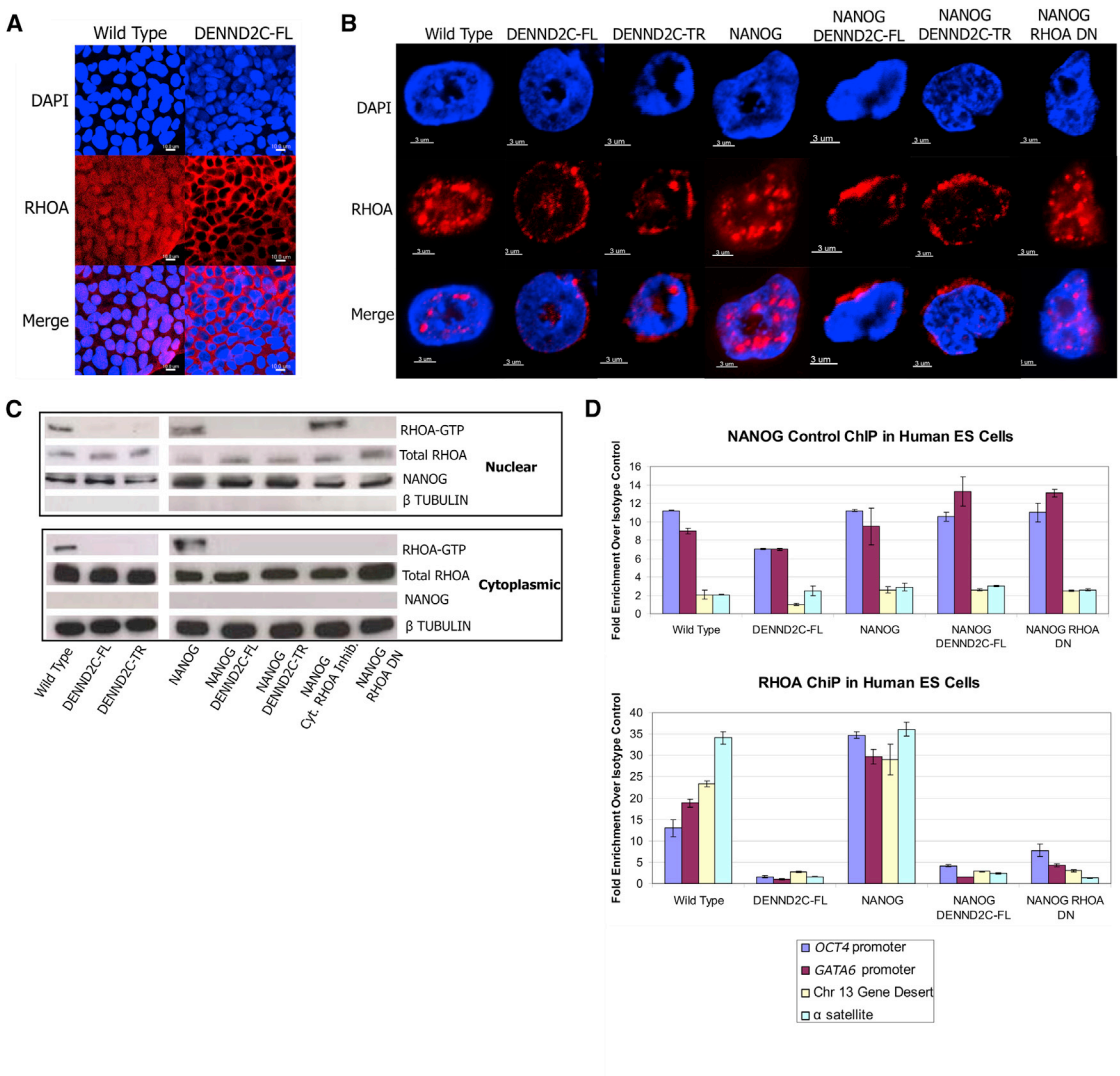

Figure 5. DENND2C Negatively Regulates Nuclear RHOA Activities

(A) DAPI and RHOA immunostaining of WT and DENND2C expressing ES cell colonies. Scale bar represents 10 μm.

(B) DAPI and RHOA immunostaining of isolated WT and DENND2C expressing nuclei. Scale bar represents 3 μm.

(C) Immunoprecipitation of active RHOA from nuclear and cytoplasmic fractions of WT and mutant cells. DENND2C and RHOA DN cells have reduced active RHOA in both nuclear and cytoplasmic fractions. Cytoplasmic RHOA inhibitor (RAB35) is included as a negative control.

(D) ChIPs performed in human ES cells with a RHOA monoclonal antibody and NANOG-positive control antibody. Presented is the average fold enrichment over IgG control of the *OCT4* promoter, *GATA6* promoter, chromosome 13 gene desert, and α satellite DNA. Error bars represent the mean percent fold enrichment over IgG control ± the SEM for triplicate technical replicates.

See Figure S3 for additional information.

centromeric α satellite DNA, indicating that RHOA does not exclusively associate with transcription units (Figure 5D). RHOA association with DNA was also confirmed in other human ES cell lines (H9 and parental H1; Figure S3I). Overall, these data show that nuclear RHOA associates with chromatin in ES cells and that this ability is affected upon downregulation of nuclear RHOA activity by DENND2C.

DISCUSSION

To date, only one genome-wide genetic screen has been performed in human ES cells (Chia et al., 2010). The high cost associated with an siRNA library can deter investigators from utilizing this approach to decipher human stem cell biology. In this study, we show that the *piggyBac* transposon can be used to conduct genetic screens in human ES cells.

The ability to rapidly and cost-effectively generate a large collection of cells in which each cell has different genes mutated by simple transfection enables one to perform phenotypic-based genetic screens in human cells in a manner similar to yeast genetics. Combined with high-throughput sequencing, the genes disrupted by the *piggyBac* transposon can be easily identified, allowing one to study the molecular mechanisms underlying any biological process.

The unique ability of the *piggyBac* transposon to carry large inserts offers the opportunity to conduct sophisticated insertional mutagenesis screens (Ding et al., 2005; Li et al., 2011). Here we were able to combine mutagenesis and simultaneous overexpression of a gene into a single transposon vector, performing a genetic screen in a sensitized background. Different from proteomic approaches, this sensitized screening strategy has the power to detect genes that cooperate in a biological process, e.g., blocking differentiation, regardless whether gene products physically interact with each other. With this strategy, we are able to probe the genome for genes capable of cooperating with NANOG, and by characterizing one of the clones, we were able to identify a poorly characterized gene, *DENND2C*, which is capable of cooperation with *NANOG* overexpression to block RA-induced differentiation. Although our *piggyBac* screen utilizes gain-of-function mutagenesis, such mutations can easily lead to the identification of loss-of-function alterations in genes in the same pathway or process, as every pathway has both positive and negative regulatory components. Indeed, we discovered that *DENND2C* is a negative regulator of RHOA. Concordantly, RHOA inactivation also cooperates with NANOG in blocking RA-induced differentiation. Although DENND2C was artificially overexpressed, we were able to phenocopy its effects with several different methods of RHOA inactivation, demonstrating that gain-of-function screens can be used to elucidate real biological mechanisms. Notably, both RHOA and DENND2C are expressed in human ES cells as well as differentiated cells and would have been missed as potential regulators of self-renewal and differentiation by more traditional approaches that focused on probing genes expressed uniquely in ES cells. Much of our understanding of RHOA comes from studies for its role in the cytoplasm as a key regulator of cytoskeleton dynamics (reviewed in Burridge and Doughman, 2006). Recently, RHOA has been found to be located within the nucleus, and its nuclear activity is stimulated by DNA damage (Dubash et al., 2011). We found that DENND2C negatively regulates the activity of nuclear RHOA in human ES cells. Furthermore, we discovered that nuclear RHOA is associated with DNA in both coding and non-coding regions and that this association is negatively regulated by DENND2C.

In summary, forward genetic analysis by *piggyBac* gain of function mutagenesis has multiple advantages complimenting genomic and biochemical methods and empowers individual investigators to functionally interrogate the human ES cell genome to elucidate mechanisms underlying biology, disease, and therapeutic strategy.

EXPERIMENTAL PROCEDURES

Cell Culture

The H1 *OCT4*-EGFP human ES cell line was created in the James Thomson laboratory and obtained from the WiCell Research Institute under the appropriate material transfer agreement (MTA). Cells were maintained on Matrigel (BD Biosciences catalog number 354277) in a 37°C incubator at 5% CO_2. Cells were passaged with manual dissociation with a 5-ml pipette after collagenase IV treatment (GIBCO catalog number 17104019) and maintained as originally described (Thomson et al., 1998). Additional information is in Supplemental Experimental Procedures.

Transfections and Drug Selection

For the screen, 9.6×10^7 human ES cells were pretreated with ROCK inhibitor as described (EMD/Calbiochem catalog number 688000; Watanabe et al., 2007) for 3 hr, dissociated with Accutase (Millipore catalog number SCR005), and split in single-cell suspension onto Matrigel coated six-well plates. Each well was treated with a cocktail consisting of 3-μg *piggyBac*, 1-μg PB transposase helper plasmid, 6-μl Fugene HD (Roche catalog number 04883560001), and 90-μl OptiMEM (Invitrogen catalog number 11058-021) for 48 hr. Cells containing stable *piggyBac* integration were selected with 1-μg/ml puromycin (Sigma catalog number P8833) starting 48 hr after transfection for a period of 2 weeks.

For transfections of all other *piggyBac* constructs, adherent human ES cells 2 days after passaging were treated with the same transfection cocktail and drug selection protocol.

RA Treatment

Human ES cells at approximately 30% confluency in six-well plates were treated with a combination of 1-μM *all-trans* RA (Sigma catalog number R2625) and 0.2-mg/ml G418 (Sigma catalog number A1720) for 8 days. Cells were then split into 10-cm plates at a ratio of two wells to one 10-cm plate. Cells were kept on G418 for another 8 days. For the screen, surviving undifferentiated colonies were individually isolated from the 10-cm plates, expanded, and retested for RA resistance. Of an initial 50 colonies isolated, only six unique clones survived this retest. For assaying resistance to differentiation, 10-cm plates were stained for the stemness marker alkaline phosphatase (Millipore catalog number SCR004).

Mapping of Insertions

Mapping was performed with a combination of linker-mediated PCR as described in Landrette et al. (2011), splinkerette PCR as described in Potter and Luo (2010) and Horn et al. (2007), and vectorette PCR as described by Carl Friddle (available at http://www.princeton.edu/genomics/botstein/protocols/vectorette.html).

PCR products created with Taq polymerase (Denville catalog number CB4050) were TOPO-TA cloned (Invitrogen catalog number 450641), and competent cells were transformed with the resulting plasmid DNA. Individual bacterial colonies carrying an insert were picked, expanded, and DNA isolated and sequenced through the Yale Keck Sequencing Facility. True insertions were separated from PCR artifacts by the identification of PBL next to the TTAA transposition site within the sequence. Sequences identified by PCR were used to identify the location and orientation of the transposon within the genome through human BLAT search (http://genome.ucsc.edu/). Additional information is in Supplemental Experimental Procedures.

Reverse Transcription and PCR

Equal amounts of total RNA was reverse transcribed using Superscript III and oligo(dT)20 (Invitrogen catalog number 18080-051). On column DNase treatment was performed as described in the instruction manual. Semiquantitative PCR was carried out in accordance with the protocol used by Darr et al. (2006). Quantitative real-time PCR was carried out on the cDNA using SYBR Green Supermix (Bio-Rad catalog number 172-5100). Samples were normalized to GAPDH amplification. Primer sequences available in Supplemental Experimental Procedures.

Active GTPase Immunoprecipitation

Immunoprecipitation of total active RHOA from 350-μg whole-cell lysate was performed with the NewEast Biosciences RhoA Activation Assay (catalog number 80601). Immunoprecipitation of active RHOA from 350-μg fractionated nuclear and cytoplasmic lysates isolated as described in Guilluy et al. (2011) was performed with the Cell Biolabs RhoA Activation Assay (catalog number STA-403-A). Immunoprecipitation of active RAC1 from 500-μg whole-cell lysate was performed with the Cell Biolabs Rac1 Activation Assay (catalog number STA-401-1).

Nuclear Isolation

The protocol is as described in Guilluy et al. (2011).

Overexpression and Mutant Constructs

All genes overexpressed in human ES cells were amplified from either human ES cell or 293T cDNA created with the Superscript III kit (Invitrogen catalog number 18080-051) with the exceptions of NANOG, which was amplified from Addgene plasmid 16578, a gift from Dr. James Thomson, and RHOA, which was amplified off Addgene plasmid 23224, a gift from Dr. Channing Der. All cDNA was amplified with MluI restriction sites and cloned into a *piggyBac* construct designed to stably overexpress the cloned gene with a β actin promoter with the sole exception of NANOG, which was overexpressed with the ubiquitin C promoter in all *PB* constructs used in this study. Dominant-negative and constitutively active constructs were created by introducing the mutations on primers and subsequent subcloning of PCR products. For assessment of cooperation with NANOG, all constructs were transfected into the same parental NANOG overexpressing cell line. Primer sequences are available in Supplemental Experimental Procedures.

ChIP

ChIP was performed using reagents from the Pierce Agarose ChIP kit (Pierce catalog number 26156), MagnaChIP Protein AG Beads (Millipore catalog number 16-663), and 6×10^6 cells (approximately two to three 10-cm plates of human ES cells) per immunoprecipitation. For each chip, we used either 2-μg NANOG antibody or rabbit IgG control (Cell Signaling catalog numbers 5232S and 2729S) or 5-μg RHOA antibody (Abcam catalog number ab54835) or mouse IgG control (Cell Signaling catalog number 5415S). Fresh chromatin and fresh antibody were incubated with 20-μl magnetic beads overnight at 4°C. Eluted chromatin was treated with RNase for 30 min prior to decrosslinking and column purification. Real-time PCR was performed in triplicate on precipitated DNA with *OCT4* promoter primers (Cell Signaling catalog number 4641S), *GATA6* promoter primers, gene desert primers (Supplemental Experimental Procedures), and α satellite repeat primers (Cell Signaling catalog number 4486S). For fold enrichment calculations, the average percentage of input DNA pulled down with NANOG, or RHOA antibody was divided by the average percentage of input DNA pulled down with the relevant IgG isotype control.

SUPPLEMENTAL INFORMATION

Supplemental Information includes Supplemental Experimental Procedures, three figures, and one table and can be found with this article online at http://dx.doi.org/10.1016/j.stemcr.2015.03.001.

ACKNOWLEDGMENTS

We thank Drs. D. Krause, J. Lu, V. Horsley, and Y. Chabu for reading the manuscript and suggestions. This study was supported in part by funding from Connecticut Stem Cell Funds and is taken from a dissertation submitted to fulfill in part the requirements for the degree of Doctor of Philosophy, Yale University. S.G. is a predoctoral student supported by National Research Service Award T32-HG003198 from the NIH, and T.X. is an HHMI investigator.

Received: December 16, 2013
Revised: March 2, 2015
Accepted: March 2, 2015
Published: April 9, 2015

REFERENCES

Allaire, P.D., Marat, A.L., Dall'Armi, C., Di Paolo, G., McPherson, P.S., and Ritter, B. (2010). The Connecdenn DENN domain: a GEF for Rab35 mediating cargo-specific exit from early endosomes. Mol. Cell *37*, 370–382.

Avilion, A.A., Nicolis, S.K., Pevny, L.H., Perez, L., Vivian, N., and Lovell-Badge, R. (2003). Multipotent cell lineages in early mouse development depend on SOX2 function. Genes Dev. *17*, 126–140.

Boyer, L.A., Lee, T.I., Cole, M.F., Johnstone, S.E., Levine, S.S., Zucker, J.P., Guenther, M.G., Kumar, R.M., Murray, H.L., Jenner, R.G., et al. (2005). Core transcriptional regulatory circuitry in human embryonic stem cells. Cell *122*, 947–956.

Buongiorno, P., Pethe, V.V., Charames, G.S., Esufali, S., and Bapat, B. (2008). Rac1 GTPase and the Rac1 exchange factor Tiam1 associate with Wnt-responsive promoters to enhance beta-catenin/TCF-dependent transcription in colorectal cancer cells. Mol. Cancer *7*, 73.

Burridge, K., and Doughman, R. (2006). Front and back by Rho and Rac. Nat. Cell Biol. *8*, 781–782.

Cai, K.Q., Capo-Chichi, C.D., Rula, M.E., Yang, D.H., and Xu, X.X. (2008). Dynamic GATA6 expression in primitive endoderm formation and maturation in early mouse embryogenesis. Dev. Dyn. *237*, 2820–2829.

Capo-Chichi, C.D., Rula, M.E., Smedberg, J.L., Vanderveer, L., Parmacek, M.S., Morrisey, E.E., Godwin, A.K., and Xu, X.X. (2005). Perception of differentiation cues by GATA factors in primitive endoderm lineage determination of mouse embryonic stem cells. Dev. Biol. *286*, 574–586.

Chambers, I., Colby, D., Robertson, M., Nichols, J., Lee, S., Tweedie, S., and Smith, A. (2003). Functional expression cloning of Nanog, a pluripotency sustaining factor in embryonic stem cells. Cell *113*, 643–655.

Chen, Y.T., Furushima, K., Hou, P.S., Ku, A.T., Deng, J.M., Jang, C.W., Fang, H., Adams, H.P., Kuo, M.L., Ho, H.N., et al. (2010). PiggyBac transposon-mediated, reversible gene transfer in human embryonic stem cells. Stem Cells Dev. *19*, 763–771.

Chevallier, J., Koop, C., Srivastava, A., Petrie, R.J., Lamarche-Vane, N., and Presley, J.F. (2009). Rab35 regulates neurite outgrowth and cell shape. FEBS Lett. *583*, 1096–1101.

Chia, N.Y., Chan, Y.S., Feng, B., Lu, X., Orlov, Y.L., Moreau, D., Kumar, P., Yang, L., Jiang, J., Lau, M.S., et al. (2010). A genome-wide RNAi screen reveals determinants of human embryonic stem cell identity. Nature *468*, 316–320.

Darr, H., Mayshar, Y., and Benvenisty, N. (2006). Overexpression of NANOG in human ES cells enables feeder-free growth while inducing primitive ectoderm features. Development *133*, 1193–1201.

de Lanerolle, P. (2012). Nuclear actin and myosins at a glance. J. Cell Sci. *125*, 4945–4949.

Ding, S., Wu, X., Li, G., Han, M., Zhuang, Y., and Xu, T. (2005). Efficient transposition of the *piggyBac* (*PB*) transposon in mammalian cells and mice. Cell *122*, 473–483.

Dubash, A.D., Guilluy, C., Srougi, M.C., Boulter, E., Burridge, K., and García-Mata, R. (2011). The small GTPase RhoA localizes to the nucleus and is activated by Net1 and DNA damage signals. PLoS ONE *6*, e17380.

Guilluy, C., Dubash, A.D., and García-Mata, R. (2011). Analysis of RhoA and Rho GEF activity in whole cells and the cell nucleus. Nat. Protoc. *6*, 2050–2060.

Hofmann, W.A. (2009). Cell and molecular biology of nuclear actin. Int Rev Cell Mol Biol *273*, 219–263.

Horn, C., Hansen, J., Schnütgen, F., Seisenberger, C., Floss, T., Irgang, M., De-Zolt, S., Wurst, W., von Melchner, H., and Noppinger, P.R. (2007). Splinkerette PCR for more efficient characterization of gene trap events. Nat. Genet. *39*, 933–934.

Jaenisch, R., and Young, R. (2008). Stem cells, the molecular circuitry of pluripotency and nuclear reprogramming. Cell *132*, 567–582.

Krawetz, R.J., Taiani, J., Greene, A., Kelly, G.M., and Rancourt, D.E. (2011). Inhibition of Rho kinase regulates specification of early differentiation events in P19 embryonal carcinoma stem cells. PLoS ONE *6*, e26484.

Landrette, S.F., Cornett, J.C., Ni, T.K., Bosenberg, M.W., and Xu, T. (2011). piggyBac transposon somatic mutagenesis with an activated reporter and tracker (PB-SMART) for genetic screens in mice. PLoS ONE *6*, e26650.

Li, M.A., Turner, D.J., Ning, Z., Yusa, K., Liang, Q., Eckert, S., Rad, L., Fitzgerald, T.W., Craig, N.L., and Bradley, A. (2011). Mobilization of giant piggyBac transposons in the mouse genome. Nucleic Acids Res. *39*, e148.

Liang, J., Wan, M., Zhang, Y., Gu, P., Xin, H., Jung, S.Y., Qin, J., Wong, J., Cooney, A.J., Liu, D., and Songyang, Z. (2008). Nanog and Oct4 associate with unique transcriptional repression complexes in embryonic stem cells. Nat. Cell Biol. *10*, 731–739.

Mallanna, S.K., Ormsbee, B.D., Iacovino, M., Gilmore, J.M., Cox, J.L., Kyba, M., Washburn, M.P., and Rizzino, A. (2010). Proteomic analysis of Sox2-associated proteins during early stages of mouse embryonic stem cell differentiation identifies Sox21 as a novel regulator of stem cell fate. Stem Cells *28*, 1715–1727.

Marat, A.L., Dokainish, H., and McPherson, P.S. (2011). DENN domain proteins: regulators of Rab GTPases. J. Biol. Chem. *286*, 13791–13800.

Mazumdar, M., Sung, M.H., and Misteli, T. (2011). Chromatin maintenance by a molecular motor protein. Nucleus *2*, 591–600.

Mitsui, K., Tokuzawa, Y., Itoh, H., Segawa, K., Murakami, M., Takahashi, K., Maruyama, M., Maeda, M., and Yamanaka, S. (2003). The homeoprotein Nanog is required for maintenance of pluripotency in mouse epiblast and ES cells. Cell *113*, 631–642.

Nichols, J., Zevnik, B., Anastassiadis, K., Niwa, H., Klewe-Nebenius, D., Chambers, I., Schöler, H., and Smith, A. (1998). Formation of pluripotent stem cells in the mammalian embryo depends on the POU transcription factor Oct4. Cell *95*, 379–391.

Pan, G., and Thomson, J.A. (2007). Nanog and transcriptional networks in embryonic stem cell pluripotency. Cell Res. *17*, 42–49.

Pardo, M., Lang, B., Yu, L., Prosser, H., Bradley, A., Babu, M.M., and Choudhary, J. (2010). An expanded Oct4 interaction network: implications for stem cell biology, development, and disease. Cell Stem Cell *6*, 382–395.

Potter, C.J., and Luo, L. (2010). Splinkerette PCR for mapping transposable elements in Drosophila. PLoS ONE *5*, e10168.

Rad, R., Rad, L., Wang, W., Cadinanos, J., Vassiliou, G., Rice, S., Campos, L.S., Yusa, K., Banerjee, R., Li, M.A., et al. (2010). PiggyBac transposon mutagenesis: a tool for cancer gene discovery in mice. Science *330*, 1104–1107.

Shim, J., Lee, S.M., Lee, M.S., Yoon, J., Kweon, H.S., and Kim, Y.J. (2010). Rab35 mediates transport of Cdc42 and Rac1 to the plasma membrane during phagocytosis. Mol. Cell. Biol. *30*, 1421–1433.

Thomson, J.A., Itskovitz-Eldor, J., Shapiro, S.S., Waknitz, M.A., Swiergiel, J.J., Marshall, V.S., and Jones, J.M. (1998). Embryonic stem cell lines derived from human blastocysts. Science *282*, 1145–1147.

van den Berg, D.L., Snoek, T., Mullin, N.P., Yates, A., Bezstarosti, K., Demmers, J., Chambers, I., and Poot, R.A. (2010). An Oct4-centered protein interaction network in embryonic stem cells. Cell Stem Cell *6*, 369–381.

Wang, J., Rao, S., Chu, J., Shen, X., Levasseur, D.N., Theunissen, T.W., and Orkin, S.H. (2006). A protein interaction network for pluripotency of embryonic stem cells. Nature *444*, 364–368.

Wang, Z., Oron, E., Nelson, B., Razis, S., and Ivanova, N. (2012). Distinct lineage specification roles for NANOG, OCT4, and SOX2 in human embryonic stem cells. Cell Stem Cell *10*, 440–454.

Watanabe, K., Ueno, M., Kamiya, D., Nishiyama, A., Matsumura, M., Wataya, T., Takahashi, J.B., Nishikawa, S., Nishikawa, S., Muguruma, K., and Sasai, Y. (2007). A ROCK inhibitor permits survival of dissociated human embryonic stem cells. Nat. Biotechnol. *25*, 681–686.

Weston, L., Coutts, A.S., and La Thangue, N.B. (2012). Actin nucleators in the nucleus: an emerging theme. J. Cell Sci. *125*, 3519–3527.

Yoshimura, S., Gerondopoulos, A., Linford, A., Rigden, D.J., and Barr, F.A. (2010). Family-wide characterization of the DENN domain Rab GDP-GTP exchange factors. J. Cell Biol. *191*, 367–381.

Zhang, X., Neganova, I., Przyborski, S., Yang, C., Cooke, M., Atkinson, S.P., Anyfantis, G., Fenyk, S., Keith, W.N., Hoare, S.F., et al. (2009). A role for NANOG in G1 to S transition in human embryonic stem cells through direct binding of CDK6 and CDC25A. J. Cell Biol. *184*, 67–82.

Zwaka, T.P., and Thomson, J.A. (2003). Homologous recombination in human embryonic stem cells. Nat. Biotechnol. *21*, 319–321.

Stem Cell Reports, Volume *4*

Supplemental Information

piggyBac Insertional Mutagenesis Screen Identifies a Role for Nuclear RHOA in Human ES Cell Differentiation

Sophia Gayle, Yukun Pan, Sean Landrette, and Tian Xu

Supplemental Figure 1

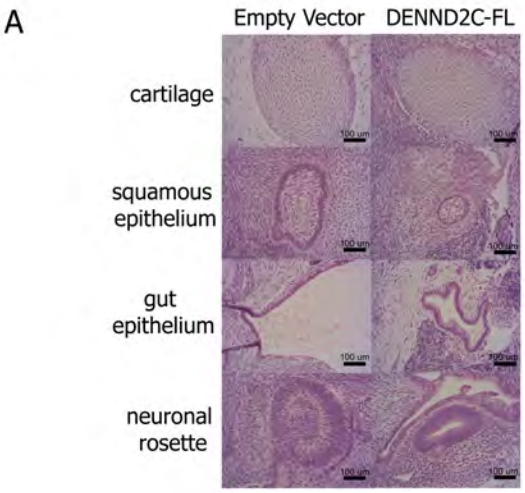

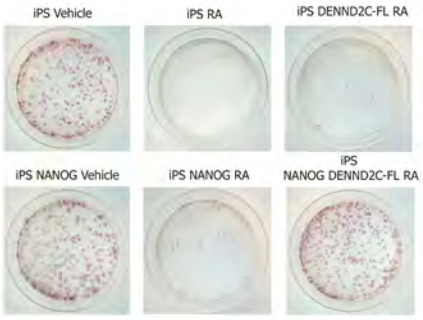

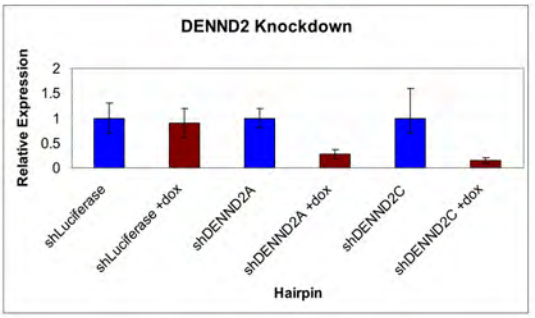

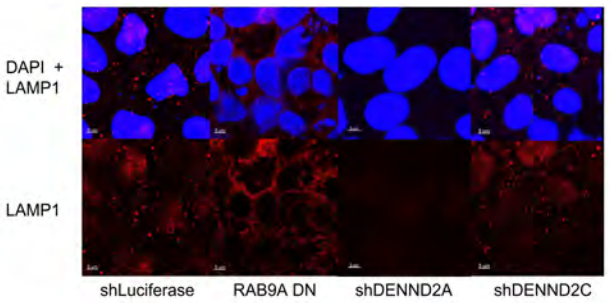

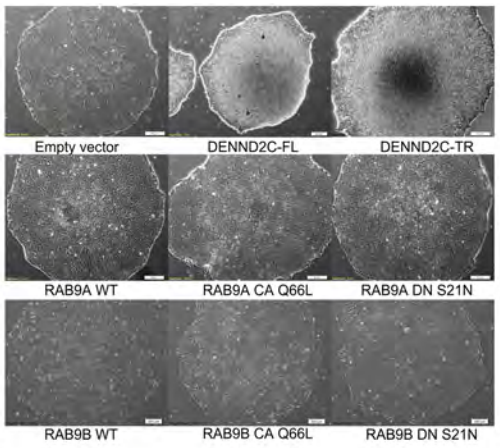

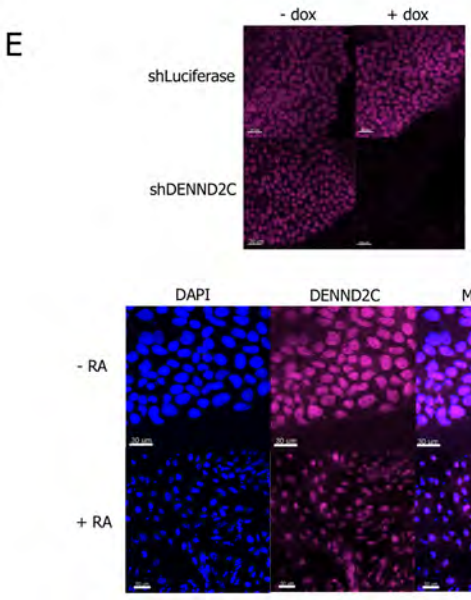

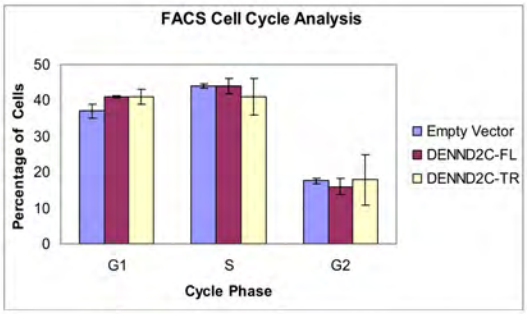

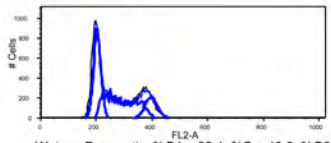

Watson Pragmatic: %G1 = 39.1; %S = 43.8; %G2 = 16.9.
Empty Vector
Event Count: 19181

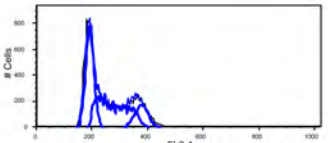

Watson Pragmatic: %G1 = 41.2; %S = 42.9; %G2 = 15.2.
DENND2C-FL
Event Count: 17980

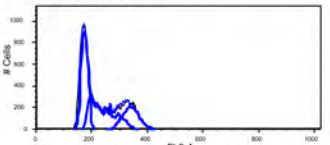

Watson Pragmatic: %G1 = 38.3; %S = 39.1; %G2 = 22.8.
DENND2C-TR
Event Count: 18308

Supplemental Figure 2

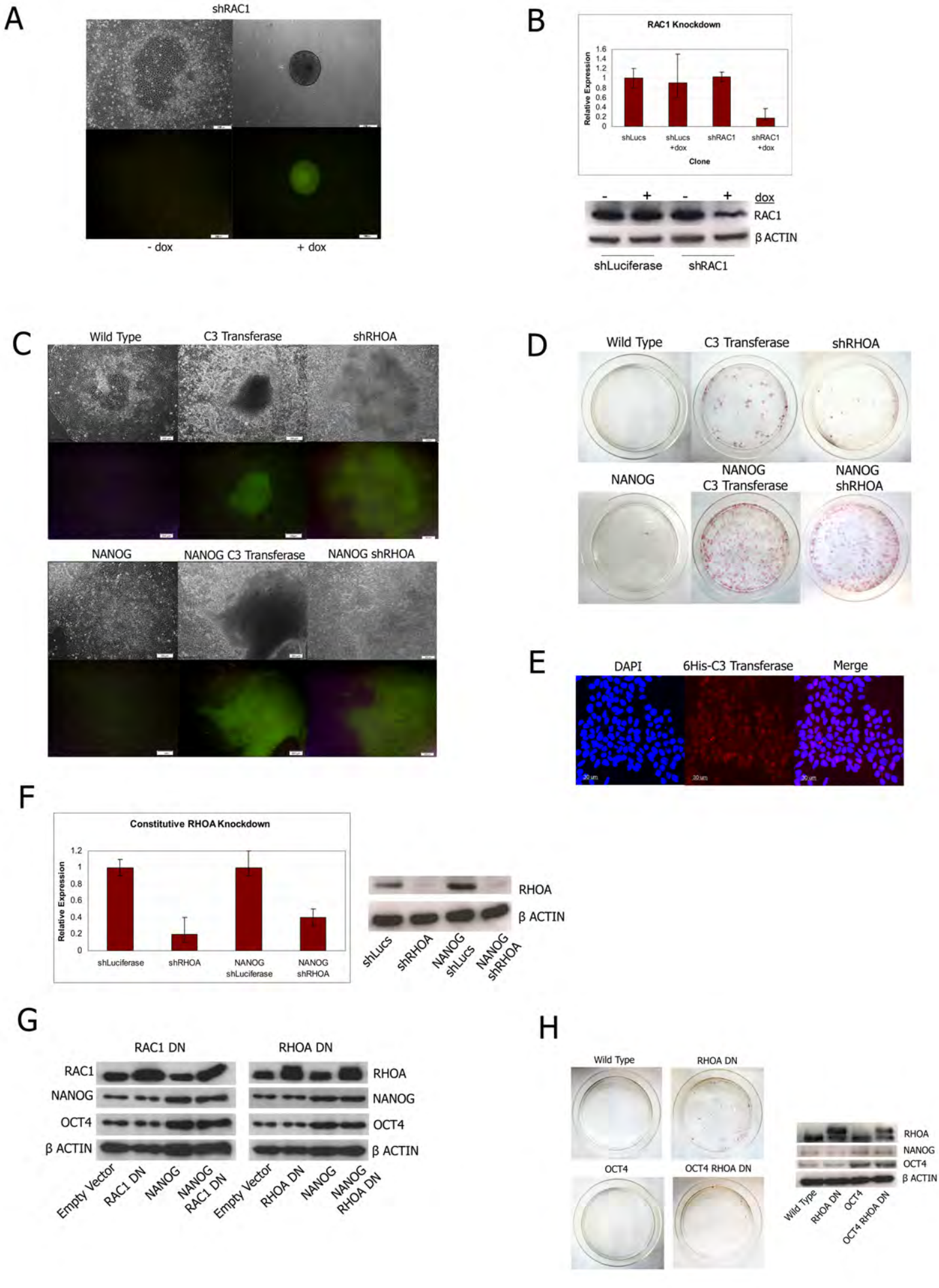

Supplemental Figure 3

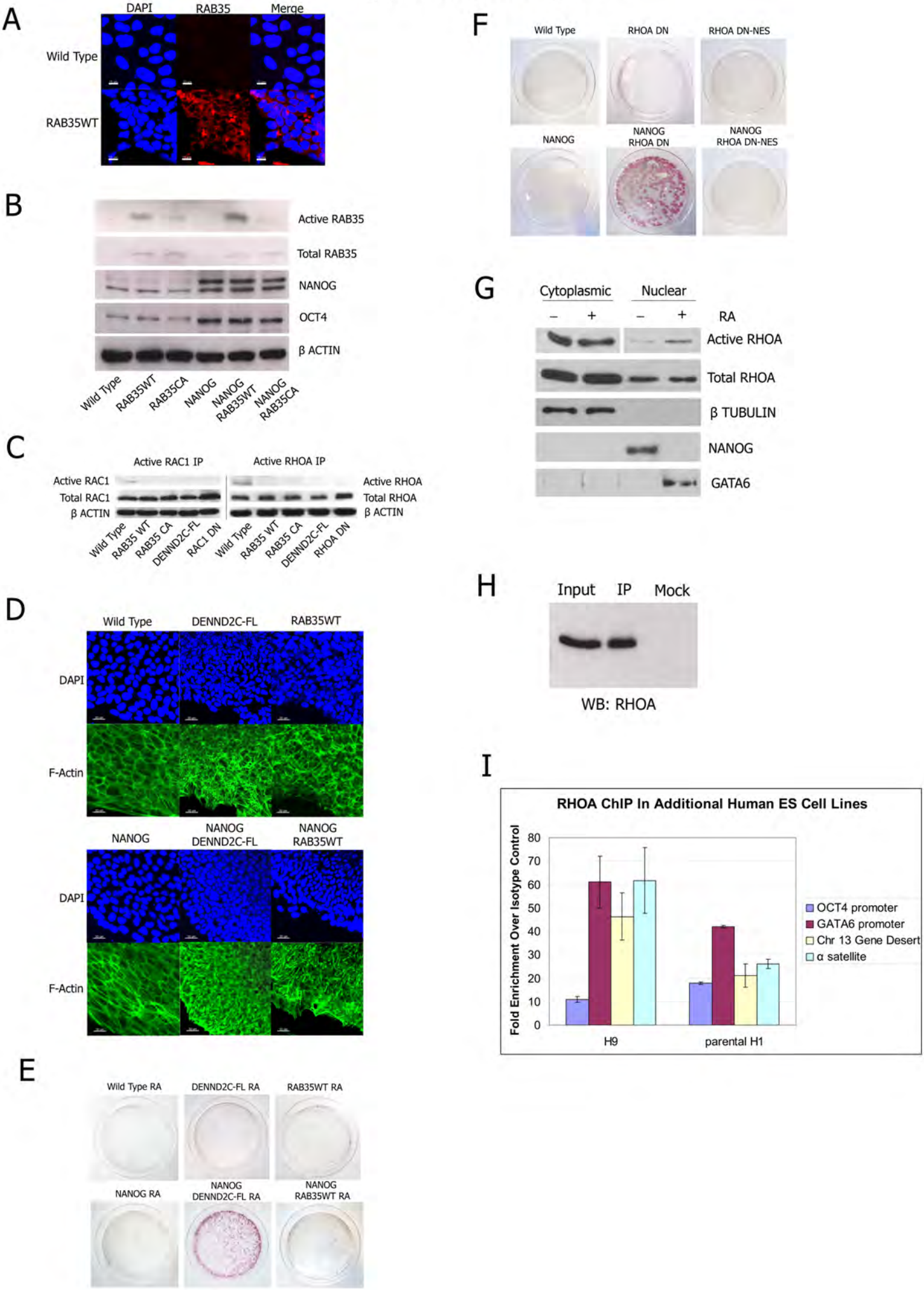

Supplemental Figure Legends

Supplemental Figure S1, related to Figure 3.

(A) Teratoma formation of empty vector and DENND2C expressing human ES cells in SCID/beige mice. Empty vector tumor formation n=5/6. DENND2C tumor formation n=10/10. Scale bar represents 100 μm.

(B) Plates containing RA differentiated induced pluripotent stem (iPS) cells stained for the stemness marker alkaline phosphatase. Experiments performed in triplicate. A representative plate is shown. Wild type RA-differentiated iPS cells are negative for strong alkaline phosphatase staining, although differentiated cells were present on the plates (not shown). Either NANOG or DENND2C-FL expression produces weak resistance of iPS cells to RA-induced differentiation. NANOG and DENND2C-FL co-expression induces enhanced resistance to RA.

(C) Top: Real time PCR results showing doxycycline inducible knockdown with a negative control hairpin targeting luciferase and hairpins targeting DENND2A and DENND2C. Mean of three technical replicates shown. Error bars represent standard deviation. Bottom: Immunostaining showing LAMP1 positive lysosomes in doxycycline treated human ES cells. Scale bar represents 5 μm.

(D) Morphology of human ES cells overexpressing DENND2C and RAB9 wild type (WT), constitutively active (CA) and dominant negative (DN) constructs within *piggyBac* vectors. All RAB9 mutants have normal colony morphology and do not phenocopy the effects of DENND2C overexpression. Scale bar represents 200 µm.

(E) Top: Immunostaining of DENND2C in wild type human ES cells bearing a doxycycline inducible hairpin targeting either luciferase or DENND2C. Scale bar represents 30 µm. Bottom: Immunostaining of DENND2C in wild type human ES cells treated with or without RA for 8 days. Scale bar represents 30 µm.

(F) Cell cycle analysis of propidum iodide-stained human ES cells containing empty *piggyBac* vector or *piggyBac* containing full length (FL) and truncated (TR) DENND2C. DENND2C overexpression does not alter cell cycle. Graph shows mean of triplicate independent experiments. Error bars represent standard deviation.

Supplemental Figure S2, related to Figure 4.

(A) Brightfield and *OCT4*-EGFP reporter images of the doxycycline inducible RAC1 knockdown human ES cell line. Induced expression of the hairpin causes cells to pile into OCT4 positive, unproliferative balls of cells after two weeks. Scale bar represents 200 μm.

(B) Real time PCR and Western blot validation of RAC1 knockdown with doxycycline inducible hairpins targeted against RAC1 and a luciferase negative control. Mean of two technical replicates shown. Error bars represent standard deviation.

(C) Brightfield and *OCT4*-EGFP reporter images of C3-Transferase treated human ES cells and RHOA knockdown cells expressing a constitutive hairpin targeted against RHOA. Cells tend to pile up into dense, large colonies that resist spontaneous differentiation at the colony center. Scale bar represents 200 μm.

(D) Alkaline phosphatase stained plates post-retinoic acid/G418 treatment. C3 Transferase treatment and RHOA knockdown cooperate with NANOG overexpression for enhanced resistance to RA-induced differentiation. Experiments performed in triplicate. A representative plate is shown.

(E) Immunostaining of human ES cells with anti-6His tag antibody to detect localization of His-tagged C3-Transferase after one week of treatment. After one week C3 Transferase is detected in the cytoplasm and is particularly enriched in the nucleus. Scale bar represents 30 μm.

(F) Real Time PCR and Western blot validating RHOA knockdown in cells constitutively expressing a hairpin targeted against RHOA. Mean of two technical replicates shown. Error bars represent standard deviation.

(G) Western blots validating overexpression of RAC1 DN and RHOA DN from stable transfection of *piggyBac* constructs. Mutant cells maintain stemness marker expression at levels compared to the parental cell lines.

(H) Left: Alkaline phosphatase stained plates post-retinoic acid/G418 treatment. OCT4 overexpression alone in human ES cells does not induce retinoic acid resistance nor does it enhance resistance of RHOA DN expressing cells. Experiments performed in triplicate. A representative plate is shown.
Right: Western blot confirming overexpression of OCT4 and RHOA DN in mutant cells. OCT4 overexpression does not induce significant NANOG overexpression.

Supplemental Figure S3, related to Figure 5.

(A) Immunostaining showing ectopic expression of cytoplasmic Rho inhibitor RAB35 in human ES cells. Wild type human ES cells do not express RAB35 by immunofluoresence. Scale bar represents 15 µm.

(B) Immunoprecipitation of active RAB35 from RAB35 expressing human ES cells. Wild type human ES cells do not appear to express RAB35. Ectopic expression of wild type RAB35 (WT) and constitutively active RAB35 Q67L (CA) results in RAB35 activation. Ectopic expression of RABWT results in greater activation of RAB35 than RAB35 CA.

(C) Ectopic expression of wild type (WT) and constitutively active (CA) RAB35 in human ES cells results in reduction of active RAC1 and RHOA in whole cell lysate similar to the effects of DENND2C overexpression.

(D) RAB35 results in small nuclear and disorganized cortical actin phenotypes similar to the effects caused by DENND2C overexpression. Scale bar represents 20 µm.

(E) Comparison of the effects of DENND2C and RAB35 on the differentiation of human ES cells. Plates stained for stemness marker alkaline phosphatase post-

retinoic acid/G418 treatment. Experiments performed in triplicate. A representative plate is shown. Unlike DENND2C, RAB35 does not cooperate with NANOG expression for enhanced resistance to retinoic acid.

(F) Comparison of the effects of RHOA DN and RHOA DN tagged with a nuclear exclusion signal (RHOA DN-NES) on the differentiation of human ES cells. Plates stained for stemness marker alkaline phosphatase post-retinoic acid/G418 treatment. Experiments performed in triplicate. A representative plate is shown. Unlike RHOA DN, RHOA DN-NES does not induce cooperation with NANOG.

(G) Immunoprecipitation of active RHOA from cytoplasmic and nuclear lysates of untreated and RA treated wild type human ES cells.

(H) Immunoprecipitation of total RHOA from whole cell lysate using a RHOA monoclonal antibody subsequently used for chIP in this study.

(I) RHOA chromatin immunoprecipitation in H9 human ES cells and the parental H1 human ES cell line from which the *OCT4*- EGFP cells were derived. RHOA is enriched on the four tested loci. Error bars represent the mean percent fold enrichment over IgG control ± the standard errors of the mean for experiments performed in triplicate.

Clone	Candidate Gene	BLAT Coordinates of PB Insertion	Function
2	*DENND2C*	chr1:115,163,248-115,163,295	Unknown
	MRE11	chr11:94,184,355-94,184,506	DNA double strand break repair
1-8	*KIAA0564*	chr13:42,217,579-42,217,700	Unknown
	CPNE8	chr12:39,337,027-39,337,404	Calcium dependent membrane binding protein
	C1S	chr12:7,147,086-7,147,235	Serine protease
	PDE4D	chr5:58316488-58316532	cAMP degradation
22	*ADARB2*	chr10:1,434,460-1,434,879	RNA editing
	ZNF429	chr19:21,519,302-21,760,301	Uncharacterized zinc finger transcription factor
25	*NINJ2*	chr12:743,116-743,227	Adhesion protein involved in nerve regeneration
	ADCY8	chr8:131,962,309-131,962,528	cAMP formation
	NPBF22P	chr5:84,954,194-85,620,860	Neuroblastoma breakpoint family, member 22, pseudogene, noncoding RNA
5	*PRDM16*	chr1:3,232,335-3,232,916	Zinc finger transcription factor, brown fat differentiation
	CASZ1	chr1:10857031-10857056	Zinc finger transcription factor, tumor suppressor involved in differentiation
8	*GABBR2*	chr9:101,113,456-101,113,544	GABA-B receptor
	HEMOGEN	chr9:101,113,456-101,113,544	Hematopoietic differentiation
	MGC70870	chr17_gl000205_random:1-171,000	C-terminal binding protein 2 pseudogene, non-coding RNA
	LINC00536	chr8:113,149,745-121,149,744	Long intergenic non-coding RNA
	GNA14	chr9:80,254,047-80,254,301	Guanine nucleotide binding protein
	GCNT2	chr6:10,528,649-10,528,776	Blood group I antigen formation
	CSF1	chr1:110,435,360-110,457,247	Macrophage differentiation

Supplemental Table S1. Candidate genes isolated from the screen.

Provided are the list of candidate genes mutagenized by PB. Insertion coordinates were provided by a BLAT search of mapped sequences adjacent to transposon ends (http://genome.ucsc.edu/).

Supplementary Experimental Procedures

Western Blotting

Whole cell extracts were prepared using lysis buffer included in NewEast Biosciences GTPase activity kits (Cat# 30303). 10-20ug of protein was used per lane in a reducing gel. Protein was transferred to nitrocellulose at 4C for 1hr at 100V and the membrane blocked with 3% BSA for 1hr at room temperature followed by overnight incubation with the appropriate antibody at 4C.

Immunofluorescence

Cells on Matrigel coated 10mm plates or isolated nuclei suspended in hypotonic solution were fixed in 4% PFA for 10 minutes, permeabilized with 0.1% Triton-X for five minutes and blocked in 0.2% goat serum for 30 minutes at room temperature. Cells were incubated with primary antibody overnight at 4C, washed and incubated with a secondary antibody for one hour at room temperature at a 1:400 dilution ratio. Stained samples were mounted with Vectashield (Vector Laboratories Cat# H-1200). Confocal images were taken in a Zeiss LSM510 Meta confocal microscope.

Antibodies

DENND2C (Abcam Cat# ab87164) 1:300 (IF)/ 1:1000 (WB)
NANOG **(**Cell Signaling Cat # 4903) 1:2000 (IF)/ 1:1000 (WB)
OCT4 (Cell Signaling Cat# 2750) 1:200 (IF) / 1:2000 (WB)
GATA6 (Cell Signaling Cat# 5851) 1:1600 (IF)/ 1:1000 (WB)
RHOA (Abcam Cat# ab54835) 1:50 (IF)/ 5:1000 (WB)

RAC1 (Cell Biolabs Cat# 240106) 1:400 (IF)/ 1:10,000 (WB)
LAMP1 (Cell Signaling Cat# 3243) 1:400 (IF)
RAB35 (NewEast Biosciences Cat# 21078) 1:200 (IF) / 1:500 (WB)
β ACTIN (Cell Signaling Cat# 3700) 1:10,000 (WB)
β TUBULIN (Sigma Cat# T3952) 1:10,000 (WB)
anti-His tag (Millipore Cat# 05-949) 1:500 (IF)
Secondary-conjugated phalloidin Invitrogen (Cat#s A22281, A12379, A12381, A22284) 1:400 (IF)

C3 Transferase (Rho Inhibitor I) and Retinoic Acid Treatment

Cells were treated with 0.1 ng/mL C3 Transferase (Cytoskeleton Inc. Cat# CT04) for one week prior to beginning retinoic acid treatment as previously described. Cells were maintained on C3 Transferase for the duration of retinoic acid treatment.

ROCK inhibitor (Y-27632) and Retinoic Acid Treatment

Cells were treated with 10uM ROCK inhibitor (SelleckBio Cat# S1049) for one week prior to beginning retinoic acid treatment as previously described. Cells were maintained on ROCK inhibitor for the duration of retinoic acid treatment.

Immmunoprecipitation

For immunoprecipitation of total RHOA, anti-RHOA beads were prepared by coupling 15ug RHOA antibody to amine reactive resin (Abcam anti-RHOA Cat# ab54835, Pierce Co-Immunoprecipitation Kit Cat# 26149). Precleared whole cell lysate containing 1 mg of protein was then incubated overnight at 4C with either 50uL RHOA conjugated resin or 50uL unconjugated resin for mock immunoprecipitation. Co-IP product was washed and eluted from resin using the Pierce kit.

Immunoprecipitation of active RAC1 from 500ug whole cell lysate was performed with the Cell Biolabs RAC1 Activation Assay (Cat# STA-401-1).
Immunoprecipitation of active RAB35 from 750ug whole cell lysate was performed with the NewEast Biosciences RAB35 Activation Assay (Cat# 82801).

Cell Culture

Induced pluripotent stem cells were derived in the laboratory of Dr. In-Hyun Park from retroviral reprogramming of human neonatal foreskin fibroblasts using OCT4, SOX2, KLF4 and C-MYC. Cells were maintained on Matrigel (BD Biosciences Cat# 354277) in a 37C incubator at 5% CO2 and passaged with manual dissociation with a 5mL pipette after collagenase IV treatment (Gibco Cat# 17104019). Cells were grown in high FGF H1 human embryonic stem cell media as prepared by the staff of Dr. Caihong Qiu at the Yale Stem Cell Core Facility. For RA treatment, cells in 6 well plates at 20% confluency were

differentiated with 1uM RA for 12 days, split 2 wells : 1 10cm plate and allowed to grow for another 8 days in normal high FGF media without RA.

The H9 and H1 human ES cell lines were obtained from the Yale Stem Cell Core from the WiCell Research Institute under the appropriate MTAs and maintained on Matrigel (BD Biosciences Cat# 354277) in a 37C incubator at 5% CO2. Cells were passaged with manual dissociation with a 5mL pipette after collagenase IV treatment (Gibco Cat# 17104019). H9 human ES cells were maintained in mTESR media (Stem Cell Technologies Cat# 05850) and H1 human ES cells were maintained in high FGF H1 human embryonic stem cell media as prepared by the staff of Dr. Caihong Qiu at the Yale Stem Cell Core Facility.

Teratoma Formation

Human ES cells were harvested by Accutase treatment (Millipore Cat# SCR005), and the pellets suspended in high FGF media with 10 uM ROCK inhibitor (Calbiochem Cat# 688000). Before injection, Matrigel (BD) was added to resuspended cells to a final concentration of 30%. 150uL of 10^7/mL cells were intramuscularly injected to the hindlimbs of a SCID/Beige mouse (Charles River). Eight weeks after injection, tumors were dissected and fixed with 10% formalin. Paraffin-embedded tissue was sliced and stained with hematoxylin and eosin. The use of human embryonic stem cells for teratoma assays was approved by Yale Embryonic Stem Cell Research Oversight (ESCRO) under protocol number E-07-019. All animal procedures were approved by the Yale Animal

Resources Center and the Institutional Animal Care and Use Committee under protocol numbers 10230.

FACS Analysis

For transfection efficiency, live cells were analyzed 48h post-transfection on a Stratedigm analyzer. For cell cycle analysis cells were fixed in cold 70% ethanol for at least 30 minutes, treated with 100uL 100ug/mL ribonuclease (Sigma Cat# R4875) and 400uL 50ug/mL propidium iodide (Sigma Cat# P4864) and data acquired on FACSCalibur. All data was analyzed using the Watson Pragmatic model on FlowJo software (Tree Star, Inc.).

Knockdown

Knockdown was performed by subcloning annealed hairpin oligos into either the Tet-pLKO-puro construct (Addgene Plasmid 21915) for doxycycline inducible expression of RAC1 or the pLKO.1-blast construct (Addgene Plasmid 26655) for constitutive repression of RHOA. Constructs were transfected into 293T cells for packaging, and virus supernatant harvested. Human ES cells were pulse infected with 1mL virus supernatant and 8ug/mL polybrene (Sigma Cat# H9268) for one hour and drug selected either with 1ug/mL puromycin or 0.1ug/mL blasticidin for two weeks 48h post-infection. Surviving Tet-pLKO-puro clones were expanded and treated with 0.5ug/mL doxycycline for 5 days to induce hairpin expression.

Hairpin sequences	
Target Gene	**Sequence**
shLuciferase	5’CCGGCGCTGAGTACTTCGAAATGTCCTCGAGGACATTT CGAAGTACTCAGCGTTTTT 3’
shDENND2A	5’CCGGCTGAAGGGACTAGGCAATAAACTCGAGTTTATTG CCTAGTCCCTTCAGTTTT 3’
shDENND2C	5’ CGGGCCTTGTTGTTGTTACATTTACTCGAGTAAATGTAA CAACAACAAGGCTTTT 3’
shRHOA	5’CCGGGAAGGATCTTCGGAATGATTCGAATCATTCCGAAG ATCCTTCTTTTTG 3’
shRAC1	5’CCGGCGCAAACAGATGTGTTCTTAACTCGAGTTAAGAAC ACATCTGTTTGCGTTTTT 3’

Primers used in this work.

Quantitative PCR Primers	
Target Gene	**Sequence**
GAPDH	F 5’AAGGTGAAGGTCGGAGTCAA 3’
	R 5’ AATGAAGGGGTCATTGATGG 3’
OCT4	F 5’ GGGTTTTTGGGATTAAGTTCTTCA 3’
	R 5’ GCCCCCACCCTTTGTGTT 3’
NANOG	F 5’ GATTTGTGGGCCTGAAGAAA 3’
	R 5’ ATGGAGGAGGGAAGAGGAGA 3’
Endogenous NANOG	F 5’ CAGTCTGGACACTGGCTGAA 3’
	R 5’ CTCGCTGATTAGGCTCCAAC 3’
REX1	F 5’ TCACAGTCCAGCAGGTGTTTG 3’
	R 5’ TCTTGTCTTTGCCCGTTTCT 3’
SOX2	F 5’ CAAAAATGGCCATGCAGGTT 3’
	R 5’ AGTTGGGATCGAACAAAAGCTATT 3’
GBX2	F 5’ GTAACTTCGACAAGGCGGAG 3’
	R 5’ TCAGATTGTCATCCGAGCTG 3’
NESTIN	F 5’ CTCAAGATGTCCCTCAGCCT 3’
	R 5’ GGTCCTAGGGAATTGCAGC 3’
TUBB3	F 5’ CCCAGTATGAGGGAGATCGT 3’
	R 5’ CGATGCCATGCTCATCAC 3’
OLIG1	F 5’ CCAGTGTTTTGTCGCAGAGA 3’

	R 5’ GCGGTTGGTTTTCGTTTTTA 3’
HUC	F 5’ GGCACACAAGAATGGTCACT 3’
	R 5’ CGTCAGTGGCTCCATTTGTA 3’
N-CADHERIN	F 5’ CCCACACCCTGGAGACATTG 3’
	R 5’ GCCGCTTTAAGGCCCTCA 3’
GFAP	F 5’ ATCGAGATCGCCACCTACAG 3’
	R 5’ CACCACGATGTTCCTCTTGA 3’
PAX6	F 5’ ACCCATTATCCAGATGTGTTTGCCC GAG 3’
	R 5’ ATGGTGAAGCTGGGCATAGGCGGC AG 3’
NKX2.2	F 5’ TGCCTCTCCTTCTGAACCTTG 3’
	R 5’ GCGAAATCTGCCACCAGTTG 3’
NKX6.1	F 5’ GTTCCTCCTCCTCCTCTTCCTC 3’
	R 5’ AAGATCTGCTGTCCGGAAAAAG 3’
GATA6	F 5’ GCCAACTGTCACACCACAAC 3’
	R 5’ TGGGGGAAGTATTTTTGCTG 3’
BRACHYURY	F 5’ GCGGGAAAGAGCCTCGAGTA 3’
	R 5’ TTCCCCGTTCACGTACTTCC 3’
AMPD1	F 5’ GGATTTCAGCAACAATGCCT 3’
	R 5’ TCCTGACGACCTCCTTCATC 3’
NRAS	F 5’ GCTTCCTCTGTGTATTTGCCA 3’
	R 5’ GCACCATAGGTACATCATCCG
TRIM33	F 5’ CTCCTTCTGCCTGCGCT 3’
	R 5’ ACTGGGCACCGTATTACACC 3’
BCAS2	F 5’ TGGAACTAATGTCACAGCATGG 3’
	R 5’ TGAAGTTCCTTCTGTGCGTG 3’
DENND2C C-term	F 5’ GCGGAGTCTTGGAAGCAAAATG 3’
	R 5’ GAATACTTCATGGGATCCTGACCC 3’
DENND2C N-term	F 5’ GGGAACATGGATGTTGGTTT 3’
	R 5’ TTGCAGTGGCTTCTTGACAG 3’
DENND2A	F 5’ TTCCATCCCTGACACACTCA 3’
	R 5’ CCCGACTCAGCTTCCTAGTG 3’
RAB9A	F 5’ TACCATGCAGATTTGGGACA 3’
	R 5’ TAAGCAGGCAGCAGTCAGAA 3’
RAB9B	F 5’ TGAAGGACCCTGAGCATTTC 3’
	R 5’ TTCCTCTACAGCCAGCACCT 3’
RHOA	F 5’ AAGGACCAGTTCCCAGAGGT 3’
	R 5’ GCTTTCCATCCACCTCGATA 3’
RAC1	F 5’ AACCAATGCATTTCCTGGAG 3’
	R 5’ TCCCATAAGCCCAGATTCAC 3’

Determination of *piggyBac* copy number by quantitative PCR

PiggyBac signal from genomic DNA was normalized to *β ACTIN* signal. Copy number was estimated relative to normalized signal from a control of known copy number previously established by Southern blot.

Determination of *piggyBac* Copy Number by Quantitative PCR		
Purpose	**Primer Name**	**Sequence**
Copy #	PBLRT2	F 5' TCACGCGGTCGTTATAGTTCAA 3'
		R 5' CCGTGAGGCGTGCTTGTC 3'
Control	BACTIN	F 5'TCACCCACACTGTGCCCATCTACGA 3'
		R 5' CAGCGGAACCGCTCATTGCCAATGG 3'

ChIP Primers

OCT4 promoter primers were sourced from Cell Signaling Cat# 4641S. α satellite repeat primers were sourced from Cell Signaling Cat# 4486S.

Chromosome 13 gene desert primers were chosen in a region with no coding genes within 500kb of either side of the sequence. GATA6 promoter primers were chosen from an area within a NANOG-binding region in human ES cells published by Boyer et al. 2005 that gave the highest signal in ChIPs performed with an antibody against NANOG.

ChIP Quantitative PCR Primers	
Ch 13 gene desert	F 5' GATTTTTGGCCACATGCTTC 3'
	R 5' TGGGCAAAGAACACAGACAG 3'
GATA6 promoter	F 5' TACGTGCAGAGGAAACAACG 3'
	R 5' GAGTTGAACTGGGGTGGAGA 3'

DENND2C Cloning

Full length and truncated DENND2C were amplified from human ES cell cDNA using primers containing MluI restriction sites and cloned into a *piggyBac* construct for stable overexpression.

DENND2C Overexpression Construct Primers		
Product	**Primer Name**	**Sequence**
Full Length	DENND2C-FL MLU F	5'ATTACGCGTGCCGCCACCATGGATGTTGGTTTTTCTCGTACTAC 3'
Truncated	DENND2C-TR MLU F	5'ATTACGCGTGCCGCCACCATGCTTGTATTGAAAATAGATGACATATTTGAATC 3'
_____	DENND2C MLU R	5' ATTACGCGTTCATTTCTTTTGCAGAAATTTCATTTTGC 3'

Mutant Constructs

To create mutant constructs, two mutant PCR products were amplified with phosphorylated primers from the wild type template: WT F/CA1 R and CA2 F/WT R. These PCR products were digested with MluI restriction enzyme and triple ligated into a *piggyBac* overexpression construct carrying a β Actin promoter, poly A tail and drug selection cassette. Abbreviations: wild type (WT), constitutively active (CA) and dominant negative (DN).

Mutant Primers			
Target	**Mutation**	**Primer Name**	**Sequence**
RAB9A	Wild Type	RAB9A WT F	5’ATTACGCGTGCCGCCACCATGGCAGG AAAATCATCAC TTTTTAAAGT 3’
		RAB9A WT R	5’ATTACGCGTTCAACAGCAAGATGAGC TAGGC 3’
	Q66L	RAB9A CA1 R	5’ AAGACCTGCCGTGTCCCAAATCTG 3’
		RAB9A CA2 F	5’ GAGCGATTCCGAAGCCTGAGG 3’
RAB9B	Wild Type	RAB9B WT F	5’ATTACGCGTGCCGCCACCATGAGTGGG AAATCCCTGCTCTTAAAG 3’
		RAB9B WT R	5’ATTACGCGTTTAACAGCACGAAGACCC TGCTTTG 3’
	Q66L	RAB9B CA1 R	5’ AAGCCCTGCAGTGTCCCAGATC 3’
		RAB9B CA2 F	5’GAACGTTTCAAGAGCCTTAGGACACC 3’
RHOA	Wild Type	RHOA WT F	5’ATTACGCGTGCCGCCACCATGGCTGCC ATCCGGAAGAAACTGG 3’
		RHOA WT R	5’ATTACGCGTTCACAAGACAAGGCACC CAGATTTTTTCTTCC 3’
	T19N	RHOA DN1 R	5’GTTCTTTCCACAGGCTCCATCACCAAC 3’
		RHOA DN2 F	5’TGCTTGCTCATAGTCTTCAGCAAGGAC C 3’
	NES	RHOA NES R	5’ ATTACGCGTTCAAAGACCAAGAGTAC GAAAAGCATCACGAAGCAAGACAAGGC ACCCAGATTTTTTCTTCC 3’
RAC1	Wild Type	RAC1 WT F	5’ATTACGCGTGCCGCCACCATGCAGGCC AT CAAGTGTGTGGTGG 3’
			5’ATTACGCGTTTACAACAGCAGGCATTT TCTCTTCCTCTTC 3’
	T17N	RAC1 DN1 R	5’ ATTTTTACCTACAGCTCCGTCTCCCA 3’
		RAC1 DN2 F	5’TGCCTACTGATCAGTTACACAACCAAT GC ATT 3’
RAB35	Wild Type	RAB35 WT F	5’ATTACGCGTGCCGCCACCATGGCCCGG GACTACGACCACCTCTTC 3’
		RAB35 WT R	5’ATTACGCGTTTAGCAGCAGCGTTTCTT TCGT TTACTGTTCTTCGTGAGC 3’
	Q67L	RAB35 CA1 R	5’ CAGCCCCGCTGTGTCCCAGATCTGC 3’
		RAB35 CA2 F	5’GAGCGCTTCCGCACCATCACCTCCAC 3’